RESEARCH PAPER

Development, Optimization And In Vivo Evaluation Of Transethosomal Gel Containing Febuxostat And Probenecid For Enhanced Antigout Activity.

Sugriv Ramesh Ghodake[1]*, Dr. Vaibhavkumar Arun Jagtap[2]

[1*-2]Department of Pharmaceutics, NES'S, Gangamai College of Pharmacy, Nagaon Dist:-Dhule 424005 Maharashtra, India. (Kavayitri Bahinabai Chaudhari North Maharashtra University, Jalgaon MH-425001)

Corresponding Author,

Sugriv R. Ghodake,

Department of Pharmaceutics, NES'S Gangamai College of Pharmacy, Nagaon Dist:-Dhule 424005 Maharashtra, India. (Kavayitri Bahinabai Chaudhari North Maharashtra University, Jalgaon MH-425001)

Email: sugrivghodake@gmail.com

Received: 12th Nov, 2025; Revised: 15th Dec 2025; Accepted: 19th Dec 2025; Available Online: 28th March, 2026

ABSTRACT

The present study aimed to develop, optimize, and evaluate a transethosomal gel containing Febuxostat and Probenecid for enhanced antigout activity. Ethosomal formulations were prepared using the thin-film hydration method and optimized through a Quality by Design (QbD)-based Box–Behnken design to achieve desirable vesicle size, polydispersity index, and entrapment efficiency. The optimized formulation (F5) exhibited nanosized vesicles (291 ± 12 nm), low PDI (0.21 ± 0.03), and high entrapment efficiency (82.1 ± 0.6%). The optimized ethosomal and transethosomal dispersions were incorporated into gel bases and further evaluated. In-vivo studies demonstrated that both formulations were safe, non-irritant, and well tolerated, with no signs of dermal or systemic toxicity. Skin retention studies revealed significantly higher drug deposition from vesicular gels, particularly transethosomes. In the MSU-induced gout model, the transethosomal gel (F7) showed superior therapeutic efficacy by significantly reducing ankle diameter, paw edema, pain score, and serum uric acid levels compared to ethosomal gel and standard treatment. Histopathological findings confirmed restoration of normal joint architecture with minimal inflammation in the transethosomal group. Stability studies indicated good physicochemical stability under accelerated conditions. Overall, the developed transethosomal gel demonstrated enhanced skin permeation, improved antigout efficacy, and excellent safety profile, suggesting its potential as an effective transdermal delivery system for gout management...

Keywords: Transethosomes; Ethosomes; Febuxostat; Probenecid; Gout; Transdermal drug delivery; Vesicular system; QbD optimization; Skin retention; Antigout activity.

How to cite this article: Ghodake SR, Jagtap VA., Development, Optimization And In Vivo Evaluation Of Transethosomal Gel Containing Febuxostat And Probenecid For Enhanced Antigout Activity..Int J Drug Deliv Technol. 2026;16(17s): 42-56. DOI: 10.25258/ijddt.16.17s.6

Source of support: Nil.

Conflict of interest: None

INTRODUCTION

Gout is a chronic inflammatory metabolic disorder characterized by the deposition of monosodium urate (MSU) crystals in joints and surrounding tissues, leading to severe pain, swelling, and impaired mobility. The condition arises primarily due to hyperuricemia, which results from either overproduction or under excretion of uric acid.[1] The global prevalence of gout has increased significantly in recent years due to lifestyle changes, dietary habits, and comorbid conditions such as obesity, diabetes, and cardiovascular diseases. Conventional pharmacotherapy for gout includes xanthine oxidase inhibitors like febuxostat and uricosuric agents such as probenecid, both of which act through complementary mechanisms to reduce serum uric acid levels and prevent crystal deposition.[2]

Febuxostat is a potent non-purine selective inhibitor of xanthine oxidase that reduces uric acid production, whereas probenecid enhances renal excretion of uric acid by inhibiting tubular reabsorption. Although both drugs are effective when administered orally, their long-term use is often associated with systemic side effects, gastrointestinal disturbances, and patient non-compliance. Additionally, oral delivery may result in variable bioavailability and delayed onset of action, which can limit therapeutic outcomes in acute gout conditions. Therefore, the development of alternative drug delivery strategies that can provide localized action, minimize systemic exposure, and improve patient compliance is highly desirable.[3]

Transdermal drug delivery systems (TDDS) have emerged as a promising approach for delivering drugs directly through the skin into systemic circulation or localized tissues. These systems offer several advantages, including

**Author for Correspondence: Sugriv Ramesh Ghodake*

avoidance of first-pass metabolism, sustained drug release, reduced dosing frequency, and improved patient adherence. However, the major challenge associated with transdermal delivery is the barrier function of the stratum corneum, which restricts the permeation of most therapeutic agents.

To overcome this limitation, advanced vesicular carriers such as ethosomes and transethosomes have been extensively investigated. Transethosomes are ultra-deformable lipid vesicles composed of phospholipids, ethanol, and edge activators (surfactants), which impart enhanced flexibility and permeability across the skin barrier. The presence of ethanol disrupts the lipid arrangement of the stratum corneum, while surfactants improve vesicle deformability, enabling deeper penetration into the skin layers. These unique characteristics make transethosomes highly suitable for delivering poorly permeable drugs and achieving improved therapeutic efficacy.[4]

Incorporating transethosomal dispersions into a gel base further enhances their applicability for topical administration by improving viscosity, spreadability, and residence time at the application site.[5] Transethosomal gels provide a controlled and sustained release of drugs, thereby ensuring prolonged therapeutic action and enhanced patient compliance. The combination of febuxostat and probenecid in a transethosomal gel system is expected to provide a synergistic antigout effect by simultaneously reducing uric acid production and enhancing its elimination, while minimizing systemic adverse effects.[6]

Despite the therapeutic potential of both drugs, limited research has been conducted on their combined delivery using advanced transdermal nanocarrier systems. Therefore, the present study aims to develop, optimize, and evaluate a transethosomal gel containing febuxostat and probenecid for enhanced antigout activity.

MATERIALS AND METHODS:

Materials:

Febuxostat and Probenecid, both of pharmaceutical grade, were procured from Yarrow Chem Products, Mumbai, India. Phospholipid (phosphatidylcholine) was obtained from Lipoid GmbH, Germany, and was used as the primary vesicle-forming component in the ethosomal formulation. Cholesterol, which served as a membrane stabilizer, was supplied by HiMedia Laboratories Pvt. Ltd., Mumbai, India. Ethanol (analytical grade), utilized for imparting flexibility and enhancing the skin permeation of ethosomal vesicles, was purchased from Loba Chemie Pvt. Ltd., Mumbai, India.

Preformulation Study:

Preformulation studies were conducted to evaluate the physicochemical properties of the pure drugs. Organoleptic characteristics such as color, odor, appearance, and texture were assessed visually under natural light and by manual examination. The melting point of each drug was determined using the capillary tube method with a digital melting point apparatus. Solubility analysis of Febuxostat and Probenecid was performed in various solvents, including distilled water, ethanol, methanol, acetone, and phosphate buffer (pH 7.4). An excess amount of drug was added to each solvent, followed by shaking at 25 ± 2°C for 24 hours.[7-8]

Formulation and development of ethosomes:

The ethosomal dispersion was prepared by a **hot method** using different concentrations of phospholipid (Phosphatidylcholine) (10, 15, 20 mg) and Cholesterol (10, 15, 20 mg). Wherein a combination of drugs Febuxostat and Probenecid were selected according to their dose. As reported, Febuxostat is more potent than Probenecid. A 1:4 ratio of Febuxostat: Probenecid (Equivalent to 2 mg of Febuxostat and 8 mg of Probenecid) was selected for the formulation. Further, Febuxostat: Probenecid (drug 10 mg) and Cholesterol were dispersed in ethanol as an organic phase. Simultaneously, the phosphatidylcholine was dissolved in an appropriate amount of water, consisting of an aqueous phase. The aqueous phase is then placed in a water bath at 40 °C until a colloidal suspension is obtained. At the same time, in another vessel, the ethanolic solution is heated to 40 °C and then added dropwise to the phospholipid dispersion under continuous stirring using a magnetic stirrer. In order to achieve the vesicular dispersion of Febuxostat and Probenecid, the dispersion was allowed to remain undistributed at room temperature for two hours. Then, the blend was subjected to probe sonication at 40% amplitude and 10 sec on/off cycles for 4 minutes utilizing a probe Sonicator **(Leela Sonic Industries)**. Formulations were then stored in the refrigerator until further characterization.[9-12]

Optimization of Febuxostat and Probenecid Ethosomal Formulation through QbD-enabled BBD Technique:[13-15]

Employing a QbD-enabled Box-Behnken statistical design (BBD) technique and Design Expert (Ver. 13.0; Stat-Ease., MN, USA) software, the ethosomal formulations of Febuxostat and Probenecid were improved. The DoE aids in showing how the formulation characteristics (ethanol, cholesterol, and phosphatidylcholine) affect the ethosome responses (vesicle size, PDI, and entrapment efficiency). Three independent variables with low (−1), medium (0), and high (+1) values were supplied by the Design Expert for 13 experimental runs in order to optimize the formulation. The software provided Eq. 1, which shows a quadratic model formula.

$$Y = a_0 + a_1A + a_2B + a_3C + a_{12}AB + a_{13}AC + a_{23}BC + a_{11}A^2 + a_{22}B^2 + a_{33}C^2 \ldots \textit{(Eq. 1)}.$$

Where Y depicted the responses, the intercept was described by a_0, the regression coefficients were depicted by a_1 to a_{33}, and the formulation attributes were expressed by A, B, and C for the Quadratic model.

Characterization of Optimized Ethosomal Drug Delivery System:

The optimized ethosomal formulation was characterized using various physicochemical and morphological parameters. The pH was determined using a calibrated digital pH meter after appropriate dilution to ensure compatibility with skin.[16-18] Vesicle size, polydispersity index (PDI), and zeta potential were measured by dynamic light scattering using a Zetasizer Nano ZS90, where small particle size, low PDI (<0.3), and zeta potential values above ±30 mV indicated uniformity and good stability of vesicles.[19-21] Drug content was analyzed by lysing the

ethosomal dispersion with ethanol followed by UV–Visible spectrophotometric estimation at respective λmax values.[22-24] Entrapment efficiency was determined using a centrifugation method, and the percentage of drug encapsulated within vesicles was calculated.[25-27] Morphological evaluation using scanning electron microscopy (SEM) revealed spherical and smooth vesicles, while transmission electron microscopy (TEM) confirmed vesicle size and structural integrity.[28-31] Furthermore, the optimized ethosomal dispersion was incorporated into a gel base using Carbopol 974P (2% w/w), with pH adjusted to 6.8–7.4 using triethanolamine and NaOH, followed by deaeration under vacuum to obtain a stable and homogeneous ethosomal gel.[32-33]

Ethosomal gel formulation for the optimized batch:

Carbopol was mixed with the optimized ethosome batch. Briefly, the gel was prepared using 2% w/w of carbopol-974P and agitated at high speed using a mechanical stirrer until no lumps were visible. After that, the stirring speed was lowered to break up the froth. Triethanolamine and NaOH were added to the gel to increase its pH to 6.8 to 7.4. The gel (F5) was left to stand under a vacuum for the whole night to get rid of the trapped air.[34-37]

***In-Vivo* Pharmacological Studies:**

Procurement of experimental Animals:

Healthy Wistar rats (150–200 g), of either sex and similar age, were procured from a CPCSEA-approved vendor (Global Research Solutions Pvt. Ltd., Pune, India). The animals were housed in polypropylene cages under controlled environmental conditions, including a 12-hour light–dark cycle, temperature of 22 ± 2 °C, and relative humidity of 55 ± 10%. Standard pellet diet and purified water were provided ad libitum. Prior to experimentation, animals were acclimatized for one week and monitored for health status to ensure suitability for the study.

To maintain uniformity in experimental conditions, animals were fasted overnight (12 hours) before treatment, with free access to water. All procedures were conducted in compliance with CPCSEA guidelines, and ethical approval was obtained from the Institutional Animal Ethics Committee (IAEC Approval No.: GBS/IAEC/2025_01/017), ensuring adherence to standard protocols for animal experimentation.[38-40]

Acute Dermal Toxicity Study:

The dermal safety of the developed formulations was evaluated according to OECD guideline 402. The optimized ethosomal and transethosomal gels were applied topically to the shaved dorsal region of rats at a dose of 2000 mg/kg. Animals were closely observed for the first 4 hours post-application and subsequently monitored daily for 14 days for any signs of toxicity, including erythema, edema, behavioral changes, or mortality. Body weight variations were also recorded throughout the study. The absence of adverse effects indicated that the formulations were safe for topical application.[41-45]

***In-Vivo* Skin Retention Study:**

The skin retention study was performed to assess the ability of different formulations to retain the drug within skin layers. Rats were divided into groups and treated with plain gel, ethosomal gel, and transethosomal gel. After topical application, animals were sacrificed at predetermined intervals (2, 4, 8, 12, and 24 hours). The treated skin was excised, washed, homogenized, and the drug was extracted using methanol. The samples were centrifuged and analyzed using UV spectrophotometry or HPLC to quantify drug retention. The results enabled comparison of drug accumulation across different formulations, reflecting their efficiency in dermal delivery.[46-57]

Table 1: *In-Vivo* Skin Retention Study

Group	Treatment	Route of drug administration
Group I	Untreated control (no gel)	Topical
Group II	Plain drug gel (without vesicles)	Topical
Group III	Optimized Ethosomal gel formulation (F5)	Topical
Group IV	Optimized Transethosomal gel formulation (F7)	Topical

***In-Vivo* Skin Irritation Study (Draize scoring method):[58-63]**

Skin irritation potential was evaluated using the Draize scoring method. The animals were divided into different groups, including negative control, positive control (sodium lauryl sulfate), placebo gel, and drug-loaded formulations. The formulations were applied to the shaved dorsal skin and covered with gauze. Observations were recorded at 1, 24, 48, and 72 hours for erythema and edema using a standardized scoring scale (0–4). Formulations with scores less than 2 were considered non-irritant, confirming their suitability for dermal application.

Table 2: *In-Vivo* Skin Irritation Study (Draize scoring method)

Group	Treatment	Route of drug administration
Group I	Normal saline (negative control)	Topical
Group II	0.8% Sodium Lauryl Sulfate (positive control)	Topical
Group III	Plain gel base (placebo)	Topical
Group IV	Optimized Ethosomal gel formulation (F5)	Topical
Group V	Optimized Transethosomal gel formulation (F7)	Topical

***In-vivo* antigout activity study**

Gout was experimentally induced by intra-articular injection of monosodium urate (MSU) crystals into the ankle joint of rats. Animals were divided into six groups, including normal control, disease control, standard drug (allopurinol), placebo, and test formulations. Treatment was initiated 4 hours after induction and continued for 7 days.

The therapeutic efficacy was assessed by measuring ankle diameter, paw edema volume, behavioral pain response, and serum uric acid levels. Reduction in these parameters indicated effective antigout activity of the developed formulations.[64-70]

Table 3: Experimental Design for *In-Vivo* Antigout Activity Study

Group	Treatment	Rout of drug administration
Group I	Normal control	-
Group II: Gout model	Disease control (MSU crystal injection)	Intra-articular
Group III: Positive control	Standard drug (Allopurinol)	Oral
Group IV	Placebo gel	Topical
Group V	Optimized Ethosomal gel formulation (F5)	Topical
Group VI	Optimized Transethosomal gel formulation (F7)	Topical

Each group consisted of 6 rats (n = 6). All procedures were performed under aseptic conditions and were approved by the IAEC.

Histopathological evaluation:

At the end of the treatment period, animals were sacrificed and the affected ankle joints were excised for histopathological analysis. The tissues were fixed in 10% neutral buffered formalin, decalcified using EDTA, and processed for paraffin embedding. Thin sections (4–5 µm) were prepared and stained with hematoxylin and eosin. Microscopic examination was performed to evaluate inflammatory cell infiltration, synovial hyperplasia, cartilage damage, and urate crystal deposition. Comparative analysis among groups provided insight into the therapeutic effectiveness of the formulations at the tissue level.[71-78]

Statistical Analysis:

All experimental data were expressed as mean ± standard deviation (SD) for six animals (n = 6). Statistical analysis was carried out using GraphPad Prism or SPSS software. Differences between groups were analyzed using one-way ANOVA followed by Tukey's post hoc test, while time-dependent studies were evaluated using repeated-measures ANOVA. A p-value < 0.05 was considered statistically significant. Additionally, drug release data were fitted into various kinetic models, and regression coefficients (R^2) were used to determine the best-fit model. Design Expert® software was employed for optimization and response surface analysis.

RESULT AND DISCUSSIONS:

Preformulation Studies:

Preformulation evaluation of Febuxostat and Probenecid revealed that both drugs are odorless, crystalline powders with smooth texture, indicating good physical stability. The observed melting points were consistent with reported values, confirming purity and absence of polymorphic changes. Solubility studies demonstrated poor aqueous solubility but good solubility in organic solvents such as ethanol and methanol, supporting the selection of lipid-based delivery systems like ethosomes for enhanced solubility and permeability.

Table 4: Preformulation Studies of Febuxostat and Probenecid

Parameter	Febuxostat	Probenecid
Color	Off-white	White
Odor	Odorless	Odorless
Appearance	Crystalline powder	Crystalline powder
Texture	Fine, smooth	Fine, smooth
Melting Point	205–208 °C	192–194 °C
Solubility in Water	Practically insoluble	Poorly soluble
Solubility in Ethanol	Soluble	Soluble
Solubility in Methanol	Freely soluble	Freely soluble
Solubility in Acetone	Soluble	Soluble
Solubility in Phosphate Buffer (pH 7.4)	Slightly soluble	Slightly soluble

Optimization of Febuxostat and Probenecid Ethosomal Formulation:

A total of thirteen ethosomal formulations (F1–F13) were prepared using the thin-film hydration method and optimized through a Quality by Design (QbD)-based Design of Experiments (DOE) approach. The influence of formulation variables phospholipid (A), ethanol (B), and cholesterol (C) on vesicle size (Y1), polydispersity index (Y2), and entrapment efficiency (Y3) was systematically evaluated. Statistical analysis indicated that phospholipid and cholesterol significantly affected all responses ($*p < 0.05$), whereas ethanol showed a comparatively minor effect. An increase in phospholipid and cholesterol concentration resulted in larger vesicle size and higher PDI, along with reduced entrapment efficiency.

The optimized formulation (F5), containing a 1:4 drug ratio (Febuxostat: Probenecid), 10 mg phosphatidylcholine, 3 mL ethanol, and 10 mg cholesterol, exhibited desirable characteristics, including vesicle size of 291 ± 12 nm, PDI of 0.21 ± 0.03, and entrapment efficiency of 82.1 ± 0.6%. The close agreement between predicted and experimental values (error <5%) confirmed the reliability of the model, and the optimized formulation was selected for further evaluation.

Table 5: Optimization of Febuxostat and Probenecid Ethosomal Formulation

		Formulation factors	Responses

Formulation	**Drug (1:4 ratio)** (Febuxostat: Probenecid) mg	**Phosphatidylcholine (mg)**	**Ethanol (mL)**	**Cholesterol (mg)**	**Vesicle size (nm)**	**PDI**	**Entrapment efficiency (mg)**
F1	10	10	2	15	382	0.38	73.2
F2	10	20	2	15	722	0.66	64.1
F3	10	10	4	15	327	0.29	76.7
F4	10	20	4	15	691	0.54	65.3
F5	***10***	***10***	***3***	***10***	***291***	***0.21***	***82.1***
F6	10	20	3	10	526	0.61	66.4
F7	10	10	3	20	698	0.74	73.1
F8	10	20	3	20	815	0.74	63.9
F9	10	15	2	10	348	0.28	68.9
F10	10	15	4	10	324	0.42	74.5
F11	10	15	2	20	714	0.68	68.3
F12	10	15	4	20	682	0.62	71.2
F13	10	15	3	15	369	0.34	74.9

Table 6: Independent variables levels for ethosomal formulations

Independent Variables	**Level used, actual coded**		
	Low (-1)	**Medium (0)**	**High (+1)**
A= Phosphatidylcholine (mg)	10	15	20
B= Ethanol (mL)	2	3	4
C= Cholesterol (mg)	10	15	20

Table 7: Optimization of Febuxostat and Probenecid transethosomal formulation

Formulation	**Drug (1:4 ratio) (Febuxostat: Probenecid) mg**	**Formulation factors**			**Responses**		
		Phosphatidylcholine (mg)	**Ethanol (mL)**	**Tween 80 (mL)**	**Vesicle size (nm)**	**PDI**	**Entrapment efficiency (mg)**
F1	10	10	2	1	262	0.43	79.8
F2	10	20	2	1	452	0.66	72.9
F3	10	10	4	1	198	0.24	84.3
F4	10	20	4	1	409	0.62	70.9
F5	10	10	3	0.6	210	0.26	82.1
F6	10	20	3	0.6	485	0.75	69.6
F7	***10***	***10***	***3***	***1.4***	***182***	***0.21***	***85.6***
F8	10	20	3	1.4	349	0.61	77.5
F9	10	15	2	0.6	403	0.59	73.3
F10	10	15	4	0.6	343	0.52	75.1
F11	10	15	2	1.4	329	0.48	78.2
F12	10	15	4	1.4	327	0.32	78.4
F13	10	15	3	1	312	0.35	76.5

Table 8: Independent variables levels for transethosomal formulations

Independent Variables	**Level used, actual coded**		
	Low (-1)	**Medium (0)**	**High (+1)**
A= Phosphatidylcholine (mg)	10	15	20
B= Ethanol (mL)	2	3	4
C= Tween 60 (mL)	0.6	1	1.4

Characterization of optimized Ethosomal and transethosomal formulations:

1. pH

The pH of all ethosomal formulations ranged from **6.36 to 6.52**, falling within the skin-compatible range (5.5–7.0), ensuring no skin irritation upon transdermal application. The optimized batch F5 showed a pH of **6.43 ± 0.03**, which is ideal for maintaining the stability of both drugs in the vesicular system and preventing skin discomfort.

2. Vesicle Size

Vesicle size is crucial for skin penetration efficiency. Formulations with smaller vesicle sizes generally offer enhanced skin permeability and better therapeutic response. Among all formulations, **F5 exhibited the smallest vesicle size of 291 ± 3.2 nm**, which is optimal for dermal diffusion. In contrast, F2 and F8 showed significantly larger vesicles (>700 nm), which may hinder transdermal drug delivery.

3. Zeta Potential

Zeta potential indicates the physical stability of colloidal systems. Values above ±30 mV suggest good repulsion between vesicles, reducing the likelihood of aggregation. The F5 batch demonstrated the **highest zeta potential (−38.6 ± 1.1 mV)**, confirming excellent stability. Other formulations such as F2, F4, F8, and F11 showed relatively lower values, indicating moderate stability.

4. Polydispersity Index (PDI)

PDI values below 0.3 reflect a narrow particle size distribution, indicating formulation uniformity. F5 showed the **lowest PDI (0.21 ± 0.01)**, confirming high homogeneity of vesicle size. In contrast, formulations like F2, F6, F7, and F8 exhibited higher PDI values (>0.6), suggesting a broader and less uniform size distribution, which may affect release behavior and stability.

5. Drug Content

High drug content reflects effective incorporation of active ingredients in the vesicular matrix. F5 recorded the **highest drug content** for both **Febuxostat (99.1 ± 1.5%)** and **Probenecid (98.6 ± 1.7%)**, indicating successful loading without degradation or loss. This ensures a potent formulation capable of delivering therapeutic doses efficiently.

6. Entrapment Efficiency (%)

Entrapment efficiency reflects the drug retention capacity of vesicles. F5 achieved the **highest entrapment efficiency of 82.1 ± 1.6%**, followed by F3 (76.7%) and F13 (74.9%). Formulations like F2 and F8 had lower values (<65%), likely due to larger vesicle sizes or suboptimal phospholipid ratios.

Based on the comprehensive analysis of all characterization parameters, **Formulation F5** demonstrated **optimal pH, smallest vesicle size, highest zeta potential, lowest PDI, superior drug content**, and **maximum entrapment efficiency**, confirming it as the **best-performing ethosomal formulation** for the combined transdermal delivery of Febuxostat and Probenecid. This formulation was selected for further **in vitro release studies, release kinetics, and stability assessments**.

Table 9: Characterization of Febuxostat and Probenecid Ethosomal Formulations

Formulation	pH	Vesicle Size (nm)	Zeta Potential (mV)	PDI	Drug Content (%) (FEB/PRO)	Entrapment Efficiency (%)
F1	6.41 ± 0.05	382 ± 4.7	−31.2 ± 1.2	0.38 ± 0.02	94.5 ± 1.8 / 92.3 ± 1.6	73.2 ± 1.5
F2	6.37 ± 0.04	722 ± 5.2	−28.7 ± 1.3	0.66 ± 0.03	92.8 ± 2.0 / 90.6 ± 1.9	64.1 ± 1.8
F3	6.52 ± 0.02	327 ± 3.6	−34.9 ± 1.1	0.29 ± 0.01	95.7 ± 1.5 / 93.8 ± 1.3	76.7 ± 1.3
F4	6.48 ± 0.06	691 ± 6.1	−29.5 ± 1.4	0.54 ± 0.02	93.9 ± 1.7 / 91.5 ± 1.8	65.3 ± 1.6
F5	***6.43 ± 0.03***	***291 ± 3.2***	***−38.6 ± 1.1***	***0.21 ± 0.01***	***99.1 ± 1.5 / 98.6 ± 1.7***	***82.1 ± 1.6***
F6	6.38 ± 0.04	526 ± 4.3	−30.8 ± 1.0	0.61 ± 0.02	93.2 ± 1.4 / 91.0 ± 1.6	66.4 ± 1.5
F7	6.45 ± 0.05	698 ± 5.6	−27.4 ± 1.6	0.74 ± 0.03	94.1 ± 1.9 / 92.7 ± 1.7	73.1 ± 1.2
F8	6.39 ± 0.06	815 ± 7.4	−25.2 ± 1.4	0.74 ± 0.02	91.8 ± 1.8 / 89.4 ± 1.6	63.9 ± 1.9
F9	6.47 ± 0.04	348 ± 3.9	−33.1 ± 1.2	0.28 ± 0.02	96.2 ± 1.3 / 94.2 ± 1.2	68.9 ± 1.4
F10	6.50 ± 0.03	324 ± 4.0	−36.5 ± 1.0	0.42 ± 0.01	97.5 ± 1.1 / 95.1 ± 1.4	74.5 ± 1.3
F11	6.36 ± 0.05	714 ± 5.8	−26.7 ± 1.5	0.68 ± 0.03	92.1 ± 1.7 / 90.8 ± 1.5	68.3 ± 1.6

F12	6.42 ± 0.04	682 ± 6.3	−29.1 ± 1.2	0.62 ± 0.02	93.8 ± 1.4 / 91.3 ± 1.2	71.2 ± 1.5
F13	6.44 ± 0.02	369 ± 3.8	−32.4 ± 1.3	0.34 ± 0.01	95.6 ± 1.2 / 93.4 ± 1.4	74.9 ± 1.4

(Mean ± SD, n = 3)

Table 10: Characterization of Febuxostat and Probenecid Transethosomal Formulations

Formulation	**Particle Size (nm)**	**PDI**	**Zeta Potential (mV)**	**Entrapment Efficiency (%)**	**Percentage Yield (%)**	**Febuxostat (%)**	**Probenecid (%)**	**pH**
F1	262 ± 5.1	0.43 ± 0.02	–23.4 ± 0.6	79.8 ± 1.1	82.3 ± 0.8	88.6 ± 1.2	87.2 ± 1.3	6.1 ± 0.3
F2	452 ± 4.8	0.66 ± 0.03	–25.1 ± 0.5	72.9 ± 1.3	84.1 ± 0.9	90.1 ± 1.2	88.5 ± 1.0	6.2 ± 0.7
F3	198 ± 3.7	0.24 ± 0.02	–28.2 ± 0.6	84.3 ± 1.0	85.6 ± 0.7	91.2 ± 1.7	89.6 ± 1.2	6.0 ± 0.8
F4	409 ± 5.2	0.62 ± 0.03	–30.5 ± 0.7	70.9 ± 1.2	86.8 ± 0.9	92.5 ± 1.4	91.3 ± 1.0	6.3 ± 0.2
F5	210 ± 3.4	0.26 ± 0.01	–26.7 ± 0.6	82.1 ± 1.1	87.4 ± 0.6	93.0 ± 1.3	92.1 ± 1.1	6.2 ± 0.3
F6	485 ± 6.2	0.75 ± 0.04	–29.0 ± 0.5	69.6 ± 1.4	88.9 ± 0.8	94.1 ± 1.7	92.8 ± 1.4	6.4 ± 0.4
F7	***182 ± 3.2***	***0.21 ± 0.01***	***–31.2 ± 0.6***	***85.6 ± 1.2***	***91.2 ± 0.9***	***95.8 ± 1.2***	***94.6 ± 1.5***	***6.2 ± 0.1***
F8	349 ± 4.5	0.61 ± 0.03	–26.5 ± 0.5	77.5 ± 1.0	89.2 ± 1.1	94.6 ± 0.6	93.1 ± 1.0	6.3 ± 0.3
F9	403 ± 4.8	0.59 ± 0.02	–27.4 ± 0.6	73.3 ± 1.1	88.3 ± 0.9	93.8 ± 0.9	92.4 ± 1.2	6.2 ± 0.7
F10	343 ± 4.2	0.52 ± 0.02	–30.1 ± 0.5	75.1 ± 1.2	90.5 ± 0.8	93.4 ± 1.8	91.9 ± 1.0	6.4 ± 0.8
F11	329 ± 4.3	0.48 ± 0.02	–25.6 ± 0.6	78.2 ± 1.0	89.0 ± 1.0	94.2 ± 1.3	93.4 ± 1.3	6.3 ± 0.1
F12	327 ± 4.0	0.32 ± 0.01	–29.3 ± 0.6	78.4 ± 1.3	87.3 ± 0.9	91.2 ± 0.9	89.8 ± 1.1	6.1 ± 0.6
F13	312 ± 3.9	0.35 ± 0.01	–23.4 ± 0.6	76.5 ± 1.2	89.6 ± 1.1	92.8 ± 1.7	91.6 ± 1.2	6.4 ± 0.5

(Mean ± SD, n = 3)

***In-vivo* Pharmacological study:**

Acute Dermal Toxicity Study: Body Weight Monitoring: Acute dermal toxicity was evaluated as per OECD guideline 402 using optimized ethosomal (F5) and transethosomal (F7) gel formulations applied at 2000 mg/kg to Wistar rats. Body weight was recorded on Day 0, 7, and 14.

Table 11: Body Weight (g) During Acute Dermal Toxicity Study

Group	**Treatment**	**Day 0**	**Day 7**	**Day 14**
A	Optimized Ethosomal gel formulation (F5)	174.3 ± 4.6	183.4 ± 4.1	191.6 ± 4.3
B	Optimized Transethosomal gel formulation (F7)	175.6 ± 3.9	182.2 ± 4.5	190.7 ± 4.0

(Mean ± SD, n = 6)

No statistically significant difference in weight gain was observed ($p > 0.05$), indicating the formulations were non-toxic.

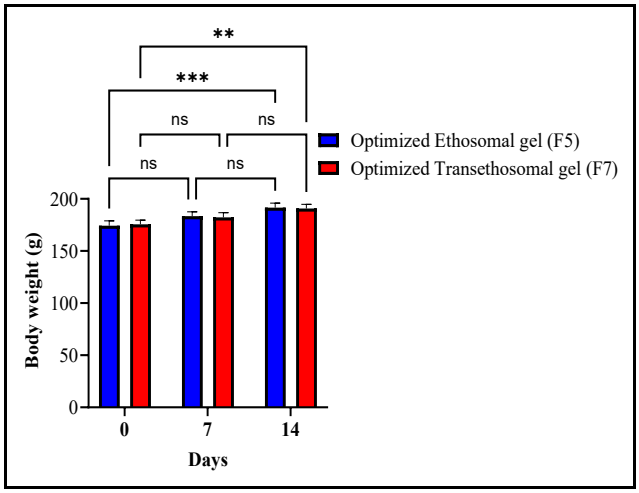

Figure 1: Body Weight (g) monitoring During Acute Dermal Toxicity Study

Dermal Toxicity Evaluation:
Animals were monitored for 14 days for signs of skin irritation such as erythema, edema, ulceration, and behavioral abnormalities. No visible signs of dermal toxicity or mortality were observed in either group, confirming the safety of both formulations for topical application.

Table 12: Dermal or skin toxicity evaluation over 14 days

Group	Formulation	Erythema	Edema	Ulceration	Mortality	Behavioral Abnormalities
A	Ethosomal gel formulation (F5)	None	None	None	None	None
B	Transethosomal gel formulation (F7)	None	None	None	None	None

The absence of dermal and systemic toxicity confirmed that the formulations were safe for topical application even at high doses.

***In-Vivo* Skin Retention Study:**
Skin retention studies demonstrated significantly higher drug deposition from vesicular formulations compared to plain gel ($p < 0.05$). Among them, the transethosomal gel (F7) showed the highest retention at all-time points, followed by ethosomal gel (F5) and plain gel. Enhanced retention is attributed to the synergistic effect of ethanol and surfactants, promoting deeper penetration and prolonged drug residence in the skin.

Table 13: Skin drug retention (µg/cm²)

Time (h)	Untreated Control	Plain Gel	Ethosomal Gel (F5)	Transethosomal Gel (F7)
2	ND	6.42 ± 0.42	10.53 ± 0.58*	12.87 ± 0.61*
4	ND	10.21 ± 0.55	18.64 ± 0.66*	22.14 ± 0.72*
8	ND	13.05 ± 0.47	26.87 ± 0.73*	31.48 ± 0.79*
12	ND	15.61 ± 0.44	29.91 ± 0.88*	35.06 ± 0.82*
24	ND	11.32 ± 0.52	24.18 ± 0.71*	28.83 ± 0.76*

*Mean ± SD (n = 6), *Values are statistically significant compared to the Plain Gel group ($p < 0.05$); ND: Not Detected*

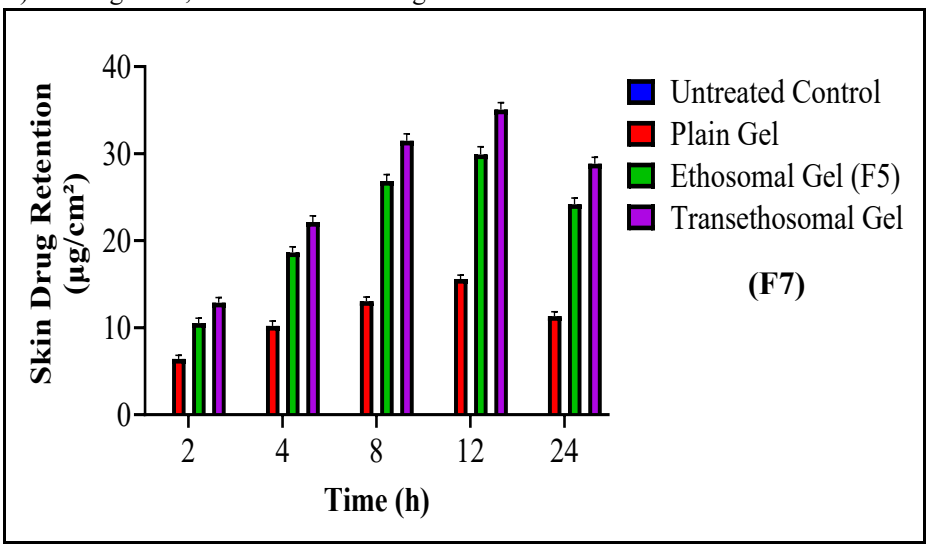

Figure 2: *In-Vivo* Skin Retention Study of ethosomal and transethosomal gel formulations

Skin Irritation Study (Draize Method):
Skin irritation potential was assessed using the Draize scoring method. Control (saline) and placebo groups showed no irritation, whereas the positive control (0.8% SLS) produced significant erythema and edema. The test formulations (F5 and F7) exhibited only mild, transient erythema during initial hours, which subsided within 72 hours, with no edema observed. The irritation scores remained below the threshold (<2), confirming the non-irritant and dermally safe nature of the developed vesicular gels.

Table 14: Skin irritation scores (Draize Method)

Group	Treatment	Erythema Score	Edema Score	Interpretation
		1h	24h	48h
I	Normal Saline (Control)	0.00 ± 0.00	0.00 ± 0.00	0.00 ± 0.00
II	0.8% Sodium Lauryl Sulfate (SLS)	2.67 ± 0.21*	3.00 ± 0.26*	2.83 ± 0.19*
III	Plain Gel Base (Placebo)	0.00 ± 0.00	0.00 ± 0.00	0.00 ± 0.00
IV	Optimized Ethosomal Gel(F5)	0.67 ± 0.11	0.33 ± 0.08	0.17 ± 0.04
V	Optimized Transethosomal Gel (F7)	0.83 ± 0.09	0.42 ± 0.07	0.25 ± 0.05

Mean ± SD, n = 6, **statistically significant compared to control group ($p < 0.05$).*

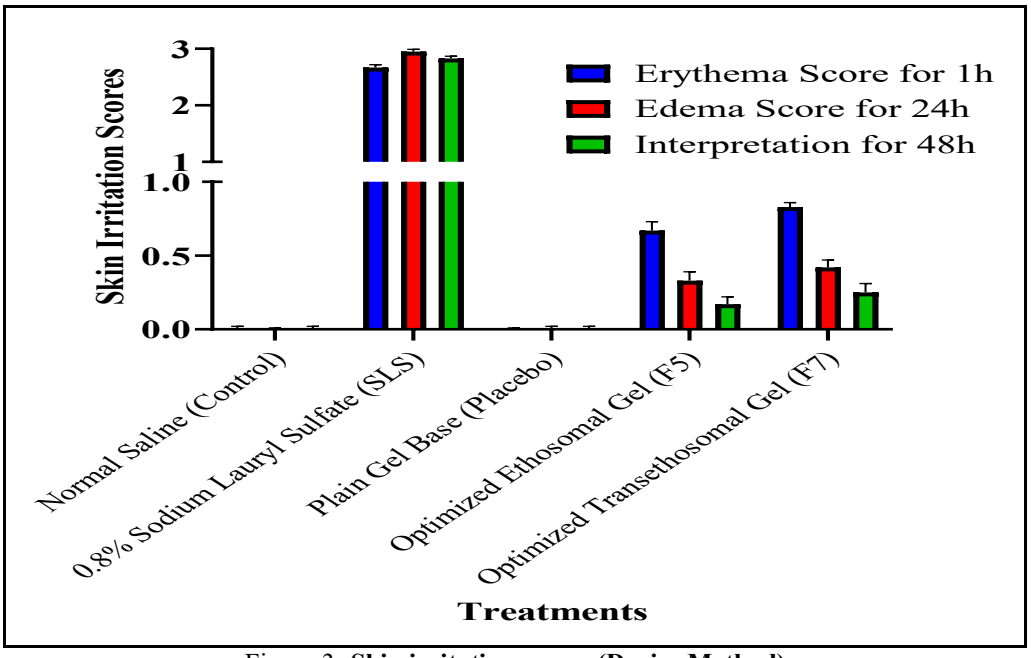

Figure 3**: Skin irritation scores (Draize Method)**

The *in-vivo* findings confirm that both ethosomal and transethosomal formulations are safe, non-toxic, and well tolerated. Furthermore, enhanced skin retention, particularly with transethosomes, highlights their superiority as effective carriers for topical delivery of Febuxostat and Probenecid, ensuring improved therapeutic performance and sustained drug action.

***In-vivo* antigout activity:**

The antigout efficacy of the developed formulations was evaluated using MSU-induced gout model in Wistar rats. The disease control group showed a significant increase in ankle diameter, paw edema, pain score, and serum uric acid levels, confirming successful induction of gout. Treatment with vesicular formulations resulted in a marked improvement in all parameters.

The optimized ethosomal gel (F5) and transethosomal gel (F7) significantly reduced ankle swelling, with F7 (5.6 ± 0.3 mm) showing greater reduction than F5 (5.9 ± 0.2 mm) and the standard allopurinol group. Similarly, paw edema volume was notably decreased in F5 (0.63 ± 0.03 mL) and F7 (0.58 ± 0.04 mL), with F7 exhibiting superior anti-inflammatory activity. Pain scores were reduced from severe (score 3) in the disease group to mild (score 1) in all treated groups, indicating effective analgesic action.

A significant reduction in serum uric acid levels was also observed, with F7 (2.8 ± 0.3 mg/dL) showing greater urate-lowering effect than F5 (3.0 ± 0.2 mg/dL) and allopurinol (3.2 ± 0.3 mg/dL). Overall, the transethosomal formulation consistently demonstrated superior therapeutic efficacy compared to ethosomal and standard treatment, highlighting its potential for effective gout management through enhanced skin penetration and sustained drug release.

Table 15: Comparative results of antigout parameters

Group	Ankle Diameter (mm)	Paw Edema Volume (mL)	Pain Score (0–4)	Serum Uric Acid (mg/dL)

Group I- Normal Control	5.2 ± 0.2	0.42 ± 0.05	0	2.4 ± 0.3
Group II – Disease Control (MSU)	7.8 ± 0.4	1.12 ± 0.06	3	5.8 ± 0.4
Group III – Standard (Allopurinol)	6.1 ± 0.3*	0.67 ± 0.04*	1*	3.2 ± 0.3*
Group IV – Placebo Gel	7.4 ± 0.3	1.05 ± 0.05	2	5.4 ± 0.5
Group V - Ethosomal Gel (F5)	5.9 ± 0.2*	0.63 ± 0.03*	1*	3.0 ± 0.2*
Group VI - Transethosomal Gel (F7)	5.6 ± 0.3*	0.58 ± 0.04*	1*	2.8 ± 0.3*

(Mean ± SD, n = 6)

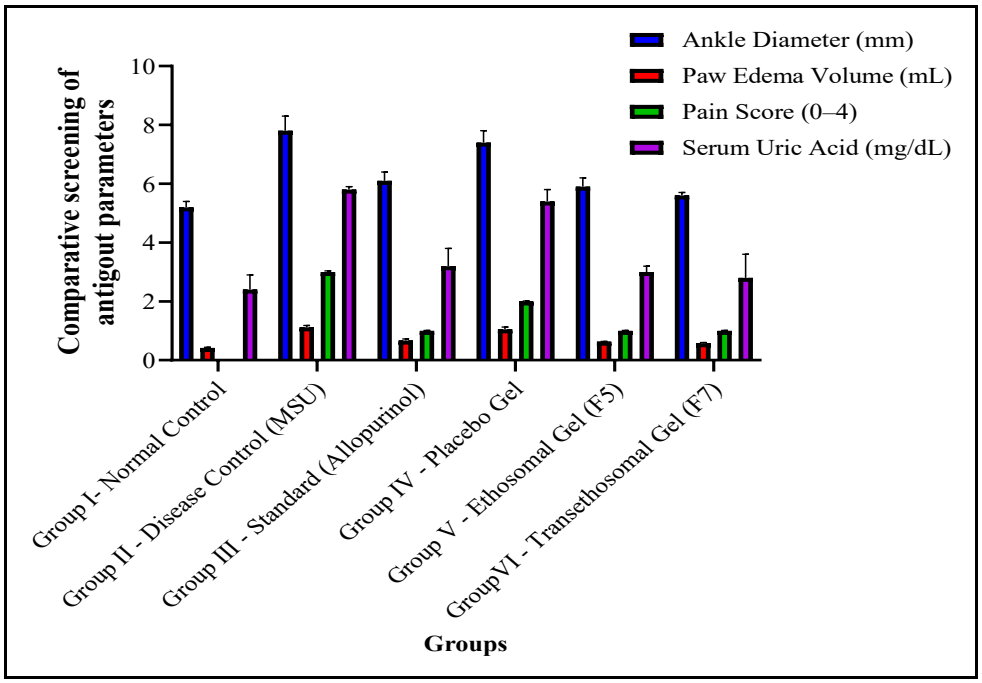

Figure 4: Comparative Results of Antigout Parameters

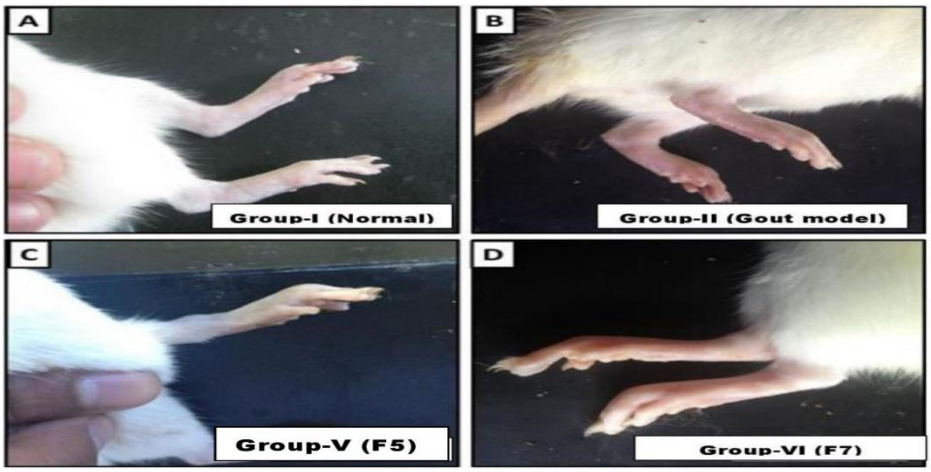

Figure 5: Effect of ethosome and transethosome formulations on MSU-induced alteration in paw morphology

Histopathological Study:

Histopathological evaluation supported the pharmacological findings. The normal control group

exhibited intact joint architecture with no signs of inflammation or crystal deposition. In contrast, the disease control group showed severe pathological alterations, including synovial hyperplasia, inflammatory cell infiltration, cartilage erosion, and extensive MSU crystal deposition.

Treatment with allopurinol showed moderate improvement, with reduced inflammation and partial restoration of joint structure. The placebo group exhibited persistent pathological changes, indicating lack of therapeutic effect. The ethosomal formulation (F5) demonstrated notable improvement with minimal inflammation and preservation of cartilage integrity.

The transethosomal formulation (F7) showed the most significant recovery, with near-normal joint architecture, negligible inflammatory infiltration, and minimal crystal deposition. These findings confirm the superior efficacy of transethosomal gel in reducing gout-induced joint damage and restoring normal histological features.

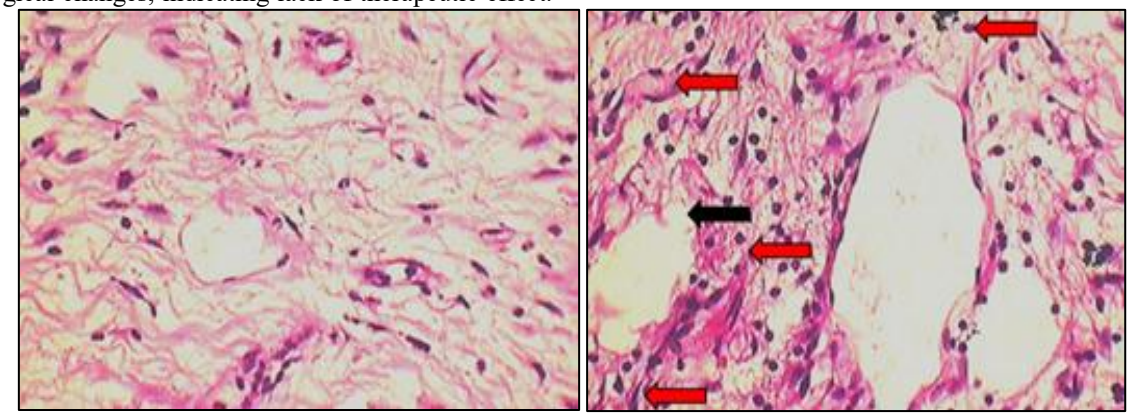

Group I – Normal Control Group II – Disease Control (MSU-Induced Gout)

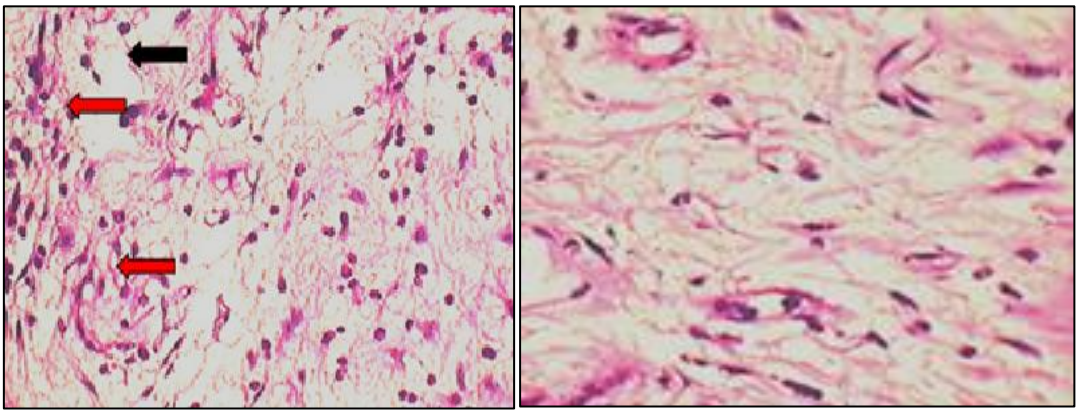

Group III – Standard Treatment (Allopurinol) Group IV – Placebo Gel

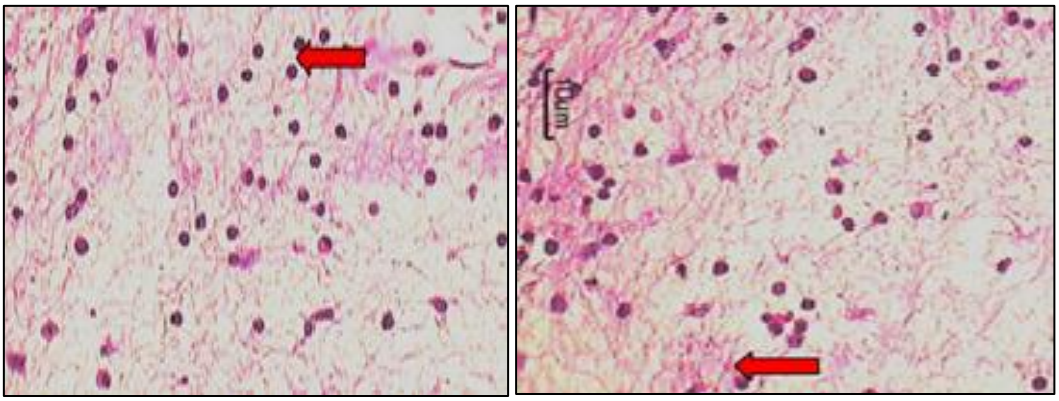

Group V – Ethosomal Formulation (F5) Group VI – Transethosomal Formulation (F7)

Figure 6: **Histopathological Study**

Stability study:

Stability studies of the optimized ethosomal (F5) and transethosomal (F7) formulations were carried out as per ICH Q1A (R2) guidelines under accelerated conditions (40 ± 2 °C/75 ± 5% RH) for 3 months. Samples were analyzed at 0, 30, 60, and 90 days for parameters including physical

appearance, pH, drug content, viscosity, entrapment efficiency, and spreadability. The results indicated no significant changes in evaluated parameters, confirming the stability and suitability of both formulations for long-term storage.

Table 16: Stability Data of Optimized Ethosomal Formulation (F5)

Time (Days)	Physical Appearance	pH (±SD)	Drug Content (%) (±SD)	Viscosity (cps) (±SD)	Entrapment Efficiency (%) (±SD)	Spreadability (g·cm/sec) (±SD)
0	Smooth, Uniform	6.2 ± 0.1	93.0 ± 1.2	3700 ± 45	73.2 ± 1.4	6.1 ± 0.2
30	No change	6.1 ± 0.1	91.8 ± 1.4	3675 ± 40	72.5 ± 1.6	6.0 ± 0.3
60	Slight dullness	6.1 ± 0.2	90.5 ± 1.6	3640 ± 55	70.9 ± 1.7	5.9 ± 0.2
90	Slight dullness	6.0 ± 0.2	88.9 ± 1.8	3600 ± 50	69.8 ± 1.9	5.8 ± 0.3

Table 17: Stability Data of Optimized Transethosomal Formulation (F7)

Time (Days)	Physical Appearance	pH (±SD)	Drug Content (%) (±SD)	Viscosity (cps) (±SD)	Entrapment Efficiency (%) (±SD)	Spreadability (g·cm/sec) (±SD)
0	Smooth, Uniform	6.1 ± 0.1	91.5 ± 1.3	3650 ± 40	71.4 ± 1.5	5.8 ± 0.2
30	No change	6.1 ± 0.1	90.4 ± 1.5	3630 ± 35	70.5 ± 1.6	5.7 ± 0.2
60	No change	6.0 ± 0.2	89.1 ± 1.7	3605 ± 50	69.3 ± 1.9	5.6 ± 0.2
90	Slight dullness	6.0 ± 0.2	87.9 ± 1.9	3580 ± 45	68.0 ± 2.0	5.5 ± 0.3

Both optimized formulations (F5 and F7) remained physically stable over 90 days, showing no significant changes in color, odor, or phase separation. Minor decreases in drug content, entrapment efficiency, viscosity, and spreadability were observed, which may be attributed to slight degradation or vesicle leakage under accelerated conditions.

The pH of both formulations remained within the acceptable dermal range (6.0–6.2), indicating good skin compatibility. Among the two, the transethosomal formulation (F7) demonstrated superior stability, retaining higher entrapment efficiency, better viscosity consistency, and more stable drug content compared to F5. These findings confirm the enhanced robustness and stability of transethosomal vesicles over conventional ethosomes.

CONCLUSION:

The present study successfully developed and optimized a transethosomal gel system for the combined delivery of Febuxostat and Probenecid. The optimized formulation exhibited favorable physicochemical characteristics, including nanosized vesicles, high entrapment efficiency, and excellent stability. *In-vivo* studies confirmed that the formulations were safe, non-irritant, and capable of enhancing drug retention within the skin. Notably, the transethosomal gel demonstrated superior antigout activity compared to ethosomal and conventional therapy by effectively reducing inflammation, pain, and serum uric acid levels. Histopathological analysis further validated its ability to restore normal joint structure. The improved performance of transethosomes can be attributed to their enhanced deformability, deeper skin penetration, and sustained drug release. Thus, the developed transethosomal gel represents a promising and effective transdermal therapeutic approach for gout management, offering improved efficacy, reduced systemic side effects, and better patient compliance.

FUNDING:

The authors declare that no funding was received for this research work.

CONFLICT OF INTEREST:

The authors declare that there is no conflict of interest regarding the publication of this paper.

REFERENCE

1. Esposito E, Drechsler M, Huang N, et al. Ethosomes and organogels for cutaneous administration of crocin. Biomed Microdevices. 2016;18(108).
2. Mao X, Cheng X, Zhang Z, et al. Therapy with ethosomes containing 5 fluorouracil for laryngotracheal stenosis in rabbit models. Eur Arch Otorhinolaryngol. 2017;274:1919–24.
3. Horwitz E, Pisanty S, Czerninski R, et al. Clinical evaluation of a novel liposomal carrier for aciclovir in recurrent herpes labialis. Oral Surg Oral Med Oral Pathol. 1999;88:700–5.
4. Lodzki M, Godin B, Rakou L, et al. Cannabidiol transdermal delivery and anti inflammatory effect in a murine model. J Control Release. 2003;93:379–389.
5. Godin B, Touitou E. Mechanism of bacitracin permeation enhancement through the skin and cellular membranes from an ethosomal carrier. J Control Release. 2004;94:365–79.
6. Godin B, Touitou E, Rubinstein E, Athamna A, Athamna M. A new approach for treatment of deep skin

infections by an ethosomal antibiotic preparation: in vivo study. J Antimicrob Chemother. 2005;55:989–94.
7. Ainbinder D, Protokin R, Chaouat M, Touitou E. Effect of honokiol and 5 FU on non melanoma skin cancer cells. J Drug Deliv Sci Technol. 2009;19:283–7.
8. Shumilov M, Touitou E. Buspirone transdermal administration for menopausal syndromes in vitro and in animal models. Int J Pharm. 2010;387:26–33.
9. Shumilov M, Bercovich R, Duchi S, et al. Ibuprofen transdermal ethosomal gel: characterization and efficacy in animal models. J Biomed Nanotechnol. 2010;6(5):569–76.
10. Ainbinder D, Touitou E. Testosterone ethosomes for enhanced transdermal delivery. Drug Deliv. 2005;12:297–303.
11. Touitou E, Godin B, Shumilov M, et al. Efficacy and tolerability of clindamycin phosphate and salicylic acid ethosomal gel in acne treatment. J Eur Acad Dermatol Venereol. 2008;22(5):629–31.
12. Ahuja N, Varma A, Pathak K. Ethosomes as vesicles for effective transdermal delivery: from bench to clinical implementation. Curr Clin Pharmacol. 2016;11:168–90.
13. Wilson V, Siram K, Rajendran S, Sankar V. Development and evaluation of finasteride-loaded ethosomes for pilosebaceous targeting. Artif Cells Nanomed Biotechnol. 2017;45(4):660–9.
14. Alghaith AF, Mahdi WA, Haq N, Alshehri S, Shakeel F. Solubility and thermodynamic properties of Febuxostat in PEG 400 + water mixtures. Materials (Basel). 2022;15(20):7318.
15. Brijesh P, Hetal T. Formulation development of fast dissolving microneedles loaded with cubosomes of Febuxostat. Pharmaceutics. 2023;15(1):224. doi:10.3390/pharmaceutics15010224.
16. Abdelbary A, Bendas ER, Ramadan AA, Mostafa DA. Pharmaceutical and pharmacokinetic evaluation of a fast dissolving flupentixol dihydrochloride film. AAPS PharmSciTech. 2014;15:1603–10.
17. Kumari MS, Prasanthi CH, Bhargavi CHS, et al. Reassessment of novel co processed multifunctional excipient. Int Res J Pharm App Sci. 2013;3:122–8.
18. Allam A, Fetih G. Sublingual fast dissolving niosomal films for metoprolol tartrate enhanced bioavailability. Drug Des Devel Ther. 2016;10:2421–33.
19. Alhakamy NA, Fahmy UA, Ahmed OAA, et al. Development of an optimized Febuxostat self nanoemulsified transdermal film: in vitro, ex vivo and in vivo evaluation. Pharm Dev Technol. 2020;25:326–31.
20. Haithem AZ, Ahmed OAA, Mohamed MA, Alhakamy NA. Febuxostat solid dispersion: development, and evaluation. Drug Dev Ind Pharm. 2022;48(10):1659–71.
21. Ahuja BK, Jena SK, Paidi SK, Bagri S, Suresh S. Febuxostat nanosuspension formulation, optimization and in vitro/in vivo evaluation. Int J Pharm. 2015;478:540–52.
22. Ketul P, Praveen K, Hetal P. Niosomal gel for enhanced transdermal lopinavir delivery vs ethosomal gel. AAPS PharmSciTech. 2012;13(4):1502–11.
23. Chourasia MK, Chan SY, Kang L, et al. Niosomal formulations for transdermal delivery of ketorolac tromethamine: in vitro, ex vivo and in vivo evaluation. J Pharm Sci. 2011;100(10):4139–52.
24. Nimmathota M, Beeravelli S, Suresh R, Jayanthi R. Pharmacokinetic and pharmacodynamic studies of etodolac-loaded vesicular gels via transdermal delivery. J Pharm Sci. 2018;107(1):255–63.
25. Guan Y, Zuo T, Chang M, Zhang F, Wei T, Shao W. Propranolol hydrochloride-loaded liposomal gel for transdermal delivery: characterization and in vivo evaluation. Int J Pharm. 2015;487:135–41.
26. Girigoswami K, Arunkumar R. Management of hypertension addressing hyperuricaemia: nano based approaches. Ann Med. 2024;56(1):2352022.
27. Sheel S, Biswas P, Karmakar V, Khanam S. Ethosome as a potential transdermal drug delivery system. J Pharm Biol Sci. 2023;10(2):72–8.
28. Manca ML, Padois K, Montis C, et al. Ethosomes: a promising drug delivery platform for transdermal application. Pharmaceutics. 2023;6(5):58.
29. Alghaith AF, Mahdi WA, Haq N, Alshehri S, Shakeel F. Solubility and thermodynamic properties of Febuxostat in PEG 400 + water mixtures. Materials (Basel). 2022;15(20):7318.
30. El-Shenawy A, Mahmoud M, Heba F, Saleh A. Torsemide fast dissolving tablets: optimization using Box–Behnken design. AAPS PharmSciTech. 2017;18:2168–79.
31. Zhang T, Sun Y, Zhang P, et al. UPLC MS/MS method for determination of Febuxostat in dog plasma: pharmacokinetic study. Biomed Chromatogr. 2013;27(2):137–41.
32. Luo Z, Nan F, Miao J, et al. Pharmacokinetics and bioequivalence of Febuxostat tablets: 4 way crossover in healthy Chinese males. Int J Biomed. 2016;1:150–61.
33. Liu X, Liu R, Ding L, et al. Pharmacokinetics of Febuxostat in healthy Chinese volunteers. Arzneimittelforschung. 2012;62(5):463–9.
34. Gide M, Sharma P, Saudagar R, Shrivastava B. Method development and validation for Febuxostat in human plasma using RP HPLC UV. Chromatogr Res Int. 2014;1:1–5.
35. OECD. (2017). Test No. 402: Acute Dermal Toxicity. OECD Publishing. https://doi.org/10.1787/9789264070585-en

36. Sayed, S., Ibrahim, H. M., & Khalil, R. M. (2020). Novel vesicular systems for enhancing dermal delivery of anti-inflammatory drugs. Colloids and Surfaces B: Biointerfaces, 190, 110948. https://doi.org/10.1016/j.colsurfb.2020.110948
37. Xu, Y., Sun, H., & Zhang, L. (2022). Histopathological evaluation in experimental models of gout: Methods and therapeutic implications. Frontiers in Immunology, 13, 872345. https://doi.org/10.3389/fimmu.2022.872345
38. Abdellatif, A. A. H., Zayed, G. M., Abourehab, M. A. S., Khames, A., & Al-Shdefat, R. (2022). Ethosomal nanocarriers as a promising platform for transdermal and dermal drug delivery: A review. Journal of Molecular Liquids, 357, 119109. https://doi.org/10.1016/j.molliq.2022.119109
39. Al Shuwaili, A. H., Rasool, B. K. A., & Abdulrasool, A. A. (2016). Optimization of elastic transfersomes formulations for transdermal delivery of pentoxifylline. European Journal of Pharmaceutical Sciences, 88, 246–256. https://doi.org/10.1016/j.ejps.2016.03.021
40. Elsayed, M. M. A., Abdallah, O. Y., Naggar, V. F., & Khalafallah, N. M. (2007). Deformable liposomes and ethosomes as carriers for skin delivery of ketotifen. Pharmaceutical Research, 24(3), 511–519. https://doi.org/10.1007/s11095-006-9171-0
41. Ghanbarzadeh, S., Arami, S., & Pourmoazzen, Z. (2015). Formulation and characterization of nanostructured lipid carriers using palm oil as a natural lipid source. Journal of Industrial and Engineering Chemistry, 22, 193–199. https://doi.org/10.1016/j.jiec.2014.07.023
42. ICH. (2003). Stability testing of new drug substances and products Q1A(R2). International Council for Harmonisation of Technical Requirements for Pharmaceuticals for Human Use. https://database.ich.org/sites/default/files/Q1A%28R2%29%20Guideline.pdf
43. Shreya, A., & Dineshmohan, V. (2018). Ethosomal gel: A novel topical drug delivery system. Journal of Drug Delivery and Therapeutics, 8(5), 385–390. https://doi.org/10.22270/jddt.v8i5.1906
44. Vaidya, V., Vyas, S., & Jain, A. (2021). Ethosomal drug delivery system: A review. International Journal of Applied Pharmaceutics, 13(4), 12–18. https://doi.org/10.22159/ijap.2021v13i4.41715
45. Sonam, B., & colleagues. (n.d.). Phytosome: Phytoconstituent based lipid derived drug delivery system. [Review of phytosome-based lipid drug delivery systems].
46. Arami, S., et al. (2013). Transdermal permeation of diclofenac sodium using conventional liposomes, ethosomes, and transfersomes. Drug Delivery, 20(8), 381–388. https://doi.org/10.3109/10717544.2013.837475
47. Kumar, R., et al. (2009). Ethosomes: Novel vesicular carriers for enhanced transdermal drug delivery. International Journal of Pharmaceutical Sciences and Research, 1(1), 1–8.
48. Chourasia, M. K., et al. (2011). Nanosized ethosomes bearing ketoprofen for improved transdermal delivery. Journal of Liposome Research, 21(4), 323–332. https://doi.org/10.3109/08982104.2011.599218
49. Li, Y., Xu, F., Li, X., Chen, S.-Y., et al. (2020). Development of curcumin-loaded composite phospholipid ethosomes for enhanced skin permeability and vesicle stability. International Journal of Pharmaceutics, 586, 119545. https://doi.org/10.1016/j.ijpharm.2020.119545
50. Michael E, Michelle A. Febuxostat: a selective xanthine Oxidase/xanthine-dehydrogenase inhibitor for the management of hyperuricemia in adults with gout. Clin Therap.2009; 31:2503–18.
51. Bishoy K, Garry G, Kenneth M, Kevin D, Richard O. Clinical pharmacokinetics and pharmacodynamics of febuxostat. Clin Pharmacokinet. 2017; 56:459–75.
52. Jain S., Umamaheshwari RB., Bhadra D., Jain NK., Ethosomes: A novel vesicular carrier for enhanced transdermal delivery of an anti-HIV agent, Indian Journal of Pharmaceutical Sciences 2004;66:72-81.
53. Touitou E., Godin B., Dayan N., Weiss C., Piliponsky A.,Levi-Schaffer F., Intracellular delivery mediated by an ethosomal carrier, Biomaterials 2001;22:3053-3059.
54. Mishra D, Mishra PK, Dabadghao S, Dubey V, Nahar M, Jain NK. Comparative evaluation of hepatitis B surface antigen-loaded elastic liposomes and ethosomes for human dendritic cell uptake and immune response. Nanomedicine: Nanotechnology, iology and Medicine 2009;6:110–8.
55. Y. Li, F. Xu, X. Li, S-Y. Chen, Development of curcumin-loaded composite phospholipid ethosomes for enhanced skin permeability and vesicle stability, International Journal of Pharmaceutics (2020)
56. Bellefroid, A. Lechanteur, B. Evrard, D. Mottet, F. Debacq-Chainiaux, G. Piel, In vitro skin penetration enhancement techniques: a combined approach of ethosomes and microneedles, International Journal of Pharmaceutics (2019),
57. El-Shenawy et al. (2020 Formulation and Characterization of Nanosized Ethosomal Formulations AAPS PharmSciTech (2020)
58. Bhupesh K. Ahuja Formulation, optimization and in vitro–in vivo evaluation of febuxostat nanosuspension International Journal of Pharmaceutics 478 (2015) 540–552.
59. A.L. Patil, Y. V. Pore, B. S. Kuchekar, S. G. Late.

Solid-state characterization and dissolution properties of bicalutamide-b-Cyclodextrins inclusion complex. Pharmazie 63. Oct 2007; 282-285.

60. Patil, Yogesh Pore, Bhanudas Kuchekar. Effect of l-Arginine on bicalutamide complexation with hydroxypropyl-β-Cyclodextrins. Digest journal of Nonmaterial's and Biostructures. June 2008; 3(2); 89-98.

61. M V Srikanth, G V Murali Mohan Babu, N Sreenivasa rao, S a Sunil, S Balaji and KV Ramanamurthy. Dissolution rate enhancement of poorly soluble bicalutamide using Cyclodextrins inclusion complexation. International journal of pharmacy and pharmaceutical research.2010; 2(1); 191-198. 58.

62. M Dixit, Rahman F, Charyalu N, Daniel S, Rasheed A, Enhancing solubility and dissolution of lovastatin by freeze drying technique. IJPRBS, 2014; Volume 3(5): 237-248.

63. M. Dixit et. al, Enhancing the aqueous solubility and dissolution of olanzapine using freeze-drying. Brazilian Journal of Pharmaceutical Sciences vol. 47, n. 4, oct. /dec., 2011.

64. A.B. Chavan V.R. Shinde, "Enhanced solubility and dissolution rate of lamotrigine by inclusion complex and solid dispersion technique." Journal of Pharmacy and pharmacology. 60 (2008) 1-9.

65. Kantilal B. Narkhede, R. B. Laware, Y. P. Sharma and S. S. Rawat. Enhancement of solubility of bicalutamide drug using solid dispersion technique. An international journal of pharmaceutical sciences. Nov 2012; 3(4); 2739-2748, 61.

66. M. V. Srikanth, B. Janaki Ram, D. Senthil Rajan, G. Adinarayana and K. V. Ramana Murthy. Dissolution rate enhancement of bicalutamide by adsorption process. African journal of pharmacy and pharmacology. June 2013; 7(21); 1357- 1362.

67. D Mudit et. al, Enhancing solubility and dissolution of indomethacin using freeze-drying. IRJP 2 (6) 2011, 69-74.

68. M. Dixit et. al, Enhancing solubility and dissolution of lovastatin using freeze-drying. IRJP 2 (6) 2014, 69-74.

69. H Sameer. Lakade1, M R Bhalekar, Freeze Drying Method for Enhancement of Solubility and Dissolution Rate of Poorly Aqueous Soluble Drug Paliperidone In Vitro–Evaluation, Am. J. Pharmtech Res. 2014; 4(1), 405-411.

70. Xu Wei-Juan et. al, in vitro dissolution and physicochemical characterizations of novel PVP-based solid dispersions containing valsartan prepared by a freeze-drying method. Pak. J. Pharm. Sci., Vol.27, No.6, November 2014, pp.1799-1804.

71. Garg, Bhawna & Garg, Neeraj & Beg, Sarwar & Singh, Bhupinder & Prakash, Om. (2015). Nanosized ethosomes-based hydrogel formulations of methoxsalen for enhanced topical delivery against vitiligo: Formulation optimization, in vitro evaluation and preclinical assessment. Journal of Drug Targeting. 24. 10.3109/1061186X.2015.1070855.

72. Abdulbaqi, I. M., Darwis, Y., Khan, N. A., Assi, R. A., & Khan, A. A. (2016). Ethosomal nanocarriers: the impact of constituents and formulation techniques on ethosomal properties, in vivo studies, and clinical trials. International journal of nanomedicine, 11, 2279–2304. https://doi.org/10.2147/IJN.S105016

73. C.K. Sudhakar, Charyulu R. Narayan, Influence of Permeation enhancer on Ethosomes bearing Lamivudine for Transdermal Drug Delivery, Research Journal of Recent Sciences, Res. J. Recent. Sci., Vol. 3(IVC-2014), 155-160 (2014).

74. Hiba Natsheh, Mohammad Qneibi, Naim Kittana, Nidal Jaradat, Mohyeddin Assali, Bahaa Shaqour, Murad Abualhasan, Abdallatif Mayyala, Yaqeen Dawoud, Tala Melhem, Sawsan Abd Alhadi, Osama Hammoudi, Abdullah Samaro, Ahmed Mousa, Sosana Bdir, Mohammad Bdair, Transethosomal system for enhanced transdermal delivery and therapeutic effect of caryophyllene oxide International Journal of Pharmaceutics, Volume 670, 2025, 125111, https://doi.org/10.1016/j.ijpharm.2024.125111.

75. Albash, R., Abdelbary, A. A., Refai, H., & El-Nabarawi, M. A. (2019). Use of transethosomes for enhancing the transdermal delivery of olmesartan medoxomil: in vitro, ex vivo, and in vivo evaluation. International journal of nanomedicine, 14, 1953–1968. https://doi.org/10.2147/IJN.S196771.

76. Bin Jardan, Y. A., Ahad, A., Raish, M., & Al-Jenoobi, F. I. (2023). Preparation and Characterization of Transethosome Formulation for the Enhanced Delivery of Sinapic Acid. Pharmaceutics, 15(10), 2391. https://doi.org/10.3390/pharmaceutics15102391

77. S. B. Gondkar, Neha R. Patil, R. B. Saudagar. Formulation Development and Characterization of Etodolac Loaded Transethosomes for Transdermal Delivery. Research J. Pharm. and Tech. 2017; 10(9): 3049-3057. doi: 10.5958/0974-360X.2017.00541.8.

78. Pratiksha n., p., priya, s., sanjana, & khandige, p. S. (2024). Transethosomes for enhanced transdermal delivery of methotrexate against rheumatoid arthritis: formulation, optimisation and characterisation. International journal of applied pharmaceutics, 16(6), 122–132. Https://doi.org/10.22159/ijap.2024v16i6.51772